Full-Sampling Focal Plane Arrays

J. R. Fisher

NRAO, P.O. Box 2, Green Bank, WV, 24944

R. F. Bradley

NRAO, 2015 Ivy Road Suite 219, Charlottesville, VA 22903-1733

Abstract.

The efficiency of single dish mapping and synthesis array mosaicing can be increased by completely sampling the information in the antenna's focal plane. This requires a densely packed array of electrically small elements. Each telescope beam is formed with a weighted combination of signals from seven or more elements. This has the added advantage of correcting for large scale reflector distortions and off-axis gain loss.

The high frequency bandwidth limit is determined by the element spacing, which must be no greater than about 0.65 to 0.9λ, depending on reflector F/D. The low frequency limit is determined by the degree to which mutual coupling can be included in the design.

We have demonstrated the feasibility of forming closely spaced beams with a low-sensitivity, 1.4 GHz, 19-element array. We will show some initial results. The array elements are now being integrated with balanced HFET amplifiers to reduce the uncooled prototype array noise temperature to about 50K. This will allow us to compare measured spillover and efficiency with our calculated values.

1. Introduction

One of the fundamental objectives of a radio telescope focal plane array for making astronomical images is to make efficient use of *all* of the information in the array's field of view. All of the heterodyne focal plane arrays built so far for radio astronomy have used conventional feed horns as array elements. This has restricted the minimum beam spacing to about two half-power beamwidths. This spacing undersamples the sky by about a factor of 16 (Johansson 1995, Padman 1995) so that as many telescope pointings are required to obtain a complete map of the field of view.

Closer beam spacing requires physically smaller array elements which, by themselves, will generally over-illuminate the telescope reflector. Spillover and taper efficiency must then be controlled by coherently combining the outputs of a number of array elements, typically seven or more, to form each beam on the sky. With approximately half-wavelength spacing of the array elements the focal plane fields are fully sampled, and there is no restriction on the minimum

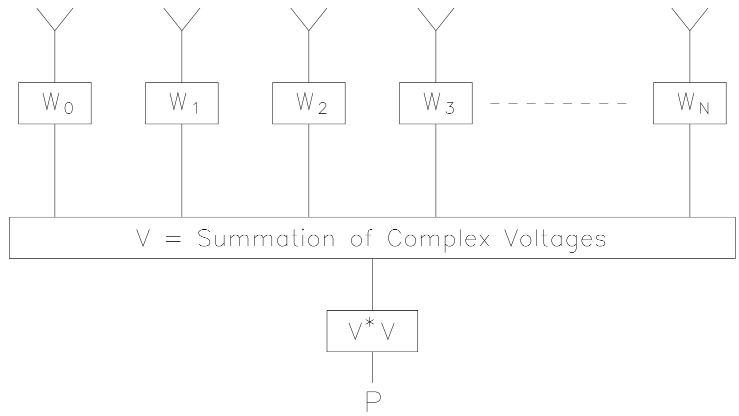

Figure 1. Direct beam-forming network for a full-sampling array feed.

beam spacing. Reuse of the amplified signal from each element to form more than one beam does not incur a sensitivity loss.

Design of an array feed then becomes a phased array problem rather than a waveguide feed design. Since the complex weights of the combined element signals may be chosen independently for each beam the array may be used to correct for large scale reflector aberrations, such as astigmatism and coma, as long as most of the power for a given beam falls on the array. In fact, cross-correlation measurements of the element signals can be used to determine the reflector distortions (Cornwell & Napier 1988).

2. Beam-Forming Networks

The main disadvantage of a full-sampling array feed is that the array requires a fairly complex beam-forming network. There are two basic network types. The direct signal combination method is shown in Figure 1. In this network the RF or IF signal voltage from each array element is given a complex (amplitude and phase) weight, W_n, before being combined with all other signals from elements that are used to form one beam on the sky. The detected power from that beam is then the square of the output of the signal combiner, or the combined signal could be used directly for further signal processing. A separate set of weights and a signal combiner are required for each beam output.

The second beam-forming method is shown in Figure 2. In this case the signals from all elements that are used to form one beam are correlated (multipled) with one another and with themselves to create a set of complex cross- and auto-correlation values. The correlation products are then given complex weights, U_{ij}, and summed to produce the beam power output. The relationship between these correlation weights and the voltage weights in Figure 1 is

$$U_{ij} = W_i \times W_j \tag{1}$$

An advantage of this correlation method is that the individual correlation products may be integrated and stored for later processing. Hence, the beam

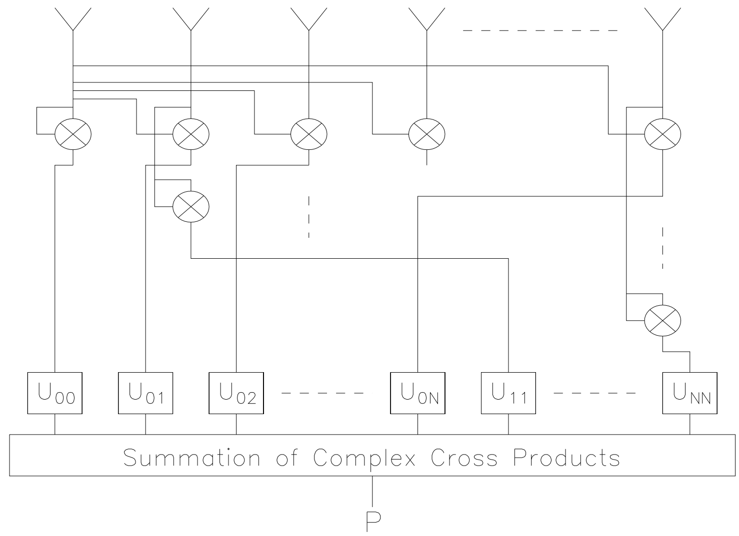

Figure 2. Correlation beam-forming network

formation may be done in software and reprocessed with various weights and optimized for different beam properties such as G/T, beam efficiency, or near-sidelobe level. A disadvantage of this method is that the correlator is expensive for arrays of practical size.

3. Element Spacing Limits

The criterion for array element spacing is that the focal plane fields be fully sampled according to the sampling theorem. Element spacing has little or nothing to do with beam spacing.

The full-sampling requirement is satisfied when there are no array grating lobe responses in the far field of the array. Since the array far field pattern is shaped to illuminate the reflector aperture this pattern and the grating responses have a finite width. Paraboloids currently in operation for radio astronomy will require prime focus arrays with patterns as wide as 140 degrees.

Figure 3 shows a one-dimensional schematic illustration of the grating responses. The horizontal coordinate is $sin(\theta)$, where θ is the angle from the array normal. In this coordinate the widths of the main and grating responses are the same and are determined by the reflector F/D. The distance between the centers of the main and grating responses is λ/s, where s is the element spacing in the same units as λ. For large F/D the acceptable spacing can approach 1λ, but for small F/D the spacing must be closer to $\lambda/2$.

The effect of the appearance of grating responses is shown in Figure 4 which plots spillover efficiency as a function of array element spacing for a hexagonally configured two-dimensional array designed for an F/D of about 0.56. The hash mark labeled S_h shows where the grating response is expected to appear in real space as the element separation is increased. The most serious effect of spillover efficiency loss is that most of the lost energy is directed toward the

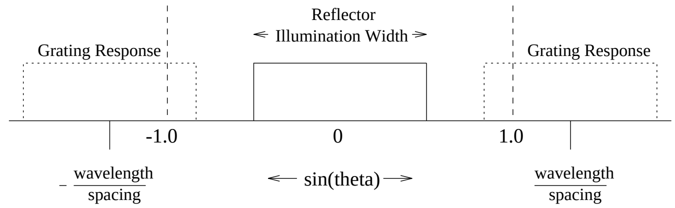

Figure 3. Schematic illustration of grating responses for the illumination of a reflector with $F/D \approx 1$. The horizontal axis is $sin(\theta)$, where θ is the angle from the array normal.

warm ground, which increases the telescope system temperature. A 1% loss of spillover efficiency corresponds to a 3 Kelvins increase in T_{sys}.

In terms of array bandwidth the element spacing limit corresponds to an upper frequency limit on an array of given dimensions. The only way to extend the array's bandwidth is to make it operate at frequencies that correspond to spacings that are small compared to a wavelength. This requires proper treatment of mutual coupling.

4. Mutual Coupling

At this point we can make only a few qualitative and empirical statements about the effects of mutual coupling on array performance. The effects of mutual coupling as a distortion of the feed patterns in horn arrays with spacings of about 2λ are well known. Spacings close to $\lambda/2$ that we require would seem catastrophic, but, in fact, this is not the case. Lower gain antennas have a smaller effective collecting area so their physical area of influence is smaller. Hence, waveguide horns with a gain of about 10 dBi should be expected to mutually interfere at about 3 times the distance of 1.5 dBi gain dipoles. The placement of dipoles or other small antennas over a ground plane tends to reduce the coupling even further because of the cancelling effect of the out-of-phase images.

Our prototype array takes a conservative approach with a spacing $> 0.5\lambda$ where measured coupling is less than -15 dB. This is not much worse than the coupling of two closely spaced horns. Bruce Veidt, of the DRAO in Penticton BC, has computed the far field patterns of the sinuous antenna embedded in an array of seven such antennas. He finds a tolerable distortion of the pattern from the free-standing element pattern. Measurement of the element patterns of our complete array is an important item on our agenda.

As long as there are no severe holes in the array pattern caused by mutual coupling within the reflector's illumination solid angle the effects of mutual coupling can be compensated by modifying the element signal weights in the beam-forming process. Whether this can be adequately done for beams near the edge of the array due to asymmetries is unclear at this point. If not, a dummy ring of elements may need to be added to the outside of the array.

It is probably worth noting that there are many arrays in operation around the world that have solved the mutual coupling problem for spacings as small as 0.1λ (e.g., Schaubert 1999).

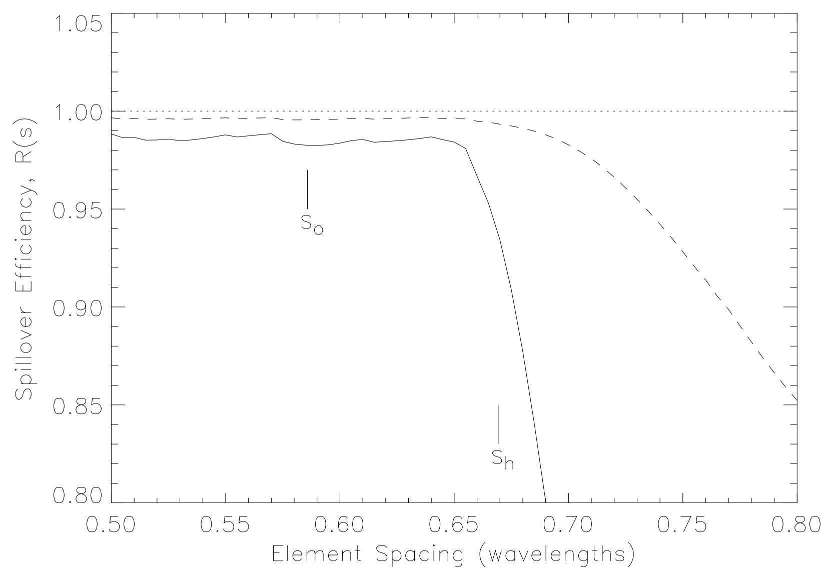

Figure 4. Spillover efficiency vs array element spacing for a two-dimensional hexagonal array designed for $F/D = 0.56$. S_0 and S_h are the angles at which grating responses are expected to enter real space ($sin(\theta) < 1$) for a rectangular and hexagonal grid array, respectively. The dash line accounts for some grating response suppression from the individual element far field pattern.

5. Initial Results

To explore the problems of a practical feed array we have constructed a 19-element prototype for test at prime focus on the 43-meter telescope in Green Bank. The array elements are sinuous antennas, which were chosen because they are inherently broadband and are inexpensive to build. These antennas are dual-linearly polarized, but our prototype array makes use of only one polarization. The array layout is shown in Figure 5. The elements are $\lambda/2$ apart at 1.16 GHz.

The receiving system is set up to cross- and self-correlate all elements in the array with a four-IF-channel FFT spectrometer having an instantaneous total bandwidth on each channel of 10 MHz. Since the spectrometer can cross- and self-correlate only two element pairs at a time, the receiver uses a crossbar IF signal switch that cycles the four spectrometer inputs through the complete combination of element pairs to measure a correlation set as illustrated in Figure 2. The product spectra are stored on disk for later processing.

To create a complete data set for investigation of the focal plane field distribution and beam formation, correlation sets were recorded with the telescope pointed at intervals of about half of a half power beamwidth (10 arcminutes) in a two-dimensional 11x11 grid around the radio source Cygnus A.

The array receiver incorporates a calibration noise source that is distributed to all 19-channels through a power splitter and a directional coupler at the input to each RF preamp. The relative phases of the signals from the array elements were calibrated with a bootstrapping process of measuring the relative phases of

Figure 5. Prototype array of 19 sinuous antennas designed to work between about 1.12 and 1.6 GHz on the 43-meter telescope.

two or three element signals when they were in the central focal plane field spot at the same time. By moving the central spot from one element pair or triplet to the next the phase calibration was carried across the array. After correcting for a slight out-of-focus phase curvature the internal phase consistency was better than about 2 degrees. Somewhat less accurate phase measurements in the lab differed by no more than 10 degrees.

Figure 6 shows the calibrated measurement of the focal plane field amplitude and phase with the radio source in the center of the field. The amplitudes relative to the central point are given by the vector length and the phase is given by the vector angle. The central eight vector lengths are truncated to better illustrate the smaller vectors. The ring shows the approximate location of the first null in the field pattern. Notice the 180-degree phase flip in the first sidelobe ring just outside of the null. The focal plane field is distorted from circular symmetry by the quadripod feed support, but we have yet to do a more detailed comparison of the measured fields with what we should expect.

Using the calibrated data, beams can be formed anywhere in the array's field of view by combining correlations as illustrated in Figure 2. Figure 7 shows superimposed maps of beams formed at various locations. Each beam used correlations from the nearest seven elements with a $sin(2\pi x)/(2\pi x)$ weighting function. A better set of weights could probably have been found in each case, but this demonstrates the idea.

6. What Next?

Our first array prototype used inexpensive RF components, and the system temperature was around 500 K. We have nearly completed design and construction

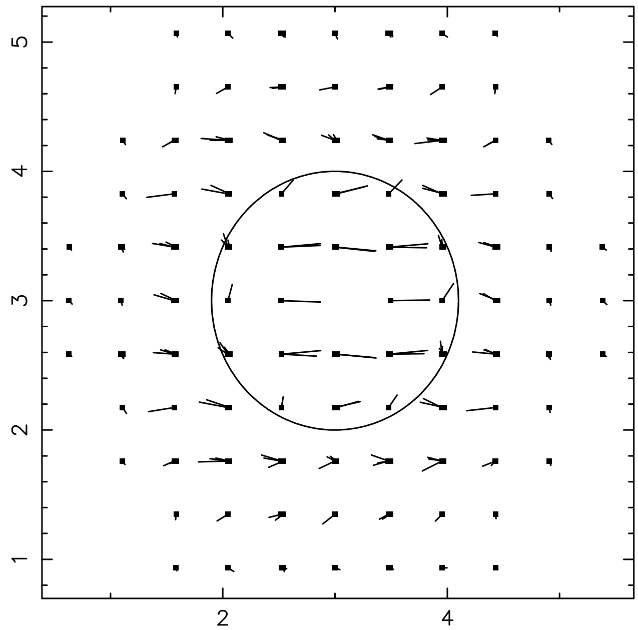

Figure 6. Measured focal plane field amplitude (vector length) and phase (vector rotation) with the radio source in the center of the field. Central vectors are truncated to 35% of the peak amplitude. Multiple vectors show the consistency of redundant measurements.

of a set of room temperature antenna/amplifier modules that will produce a system temperature af about 50 K. Tests with the new receiver on the 43-meter telescope are scheduled for September of this year. The improved sensitivity will allow us to verify our spillover calculations and examine the effects of mutual coupling. We also plan antenna range measurements of the entire array to compare with the telescope tests.

An astronomically interesting receiver will require cooled amplifier modules so we are looking into various cooling schemes.

References

Cornwell, T. J. & Napier, P. J. 1988, Radio Science, 23, 739

Johansson, J. F. 1995, 75, 82, *Multi-feed Systems for Radio Telescopes*, Eds. Emerson, D. T., Payne, J. M., Astronomical Society of the Pacific Conference Series

Padman, R. 1995, 75, 3, *Multi-feed Systems for Radio Telescopes*, Eds. Emerson, D. T., Payne, J. M., Astronomical Society of the Pacific Conference Series

Schaubert, D. 1999, "Wideband Vivaldi arrays for large aperture antennas", workshop on *Perspectives on Radio Astronomy: Technologies for Large Antenna Arrays*, Dwingeloo, The Netherlands, April 12-14

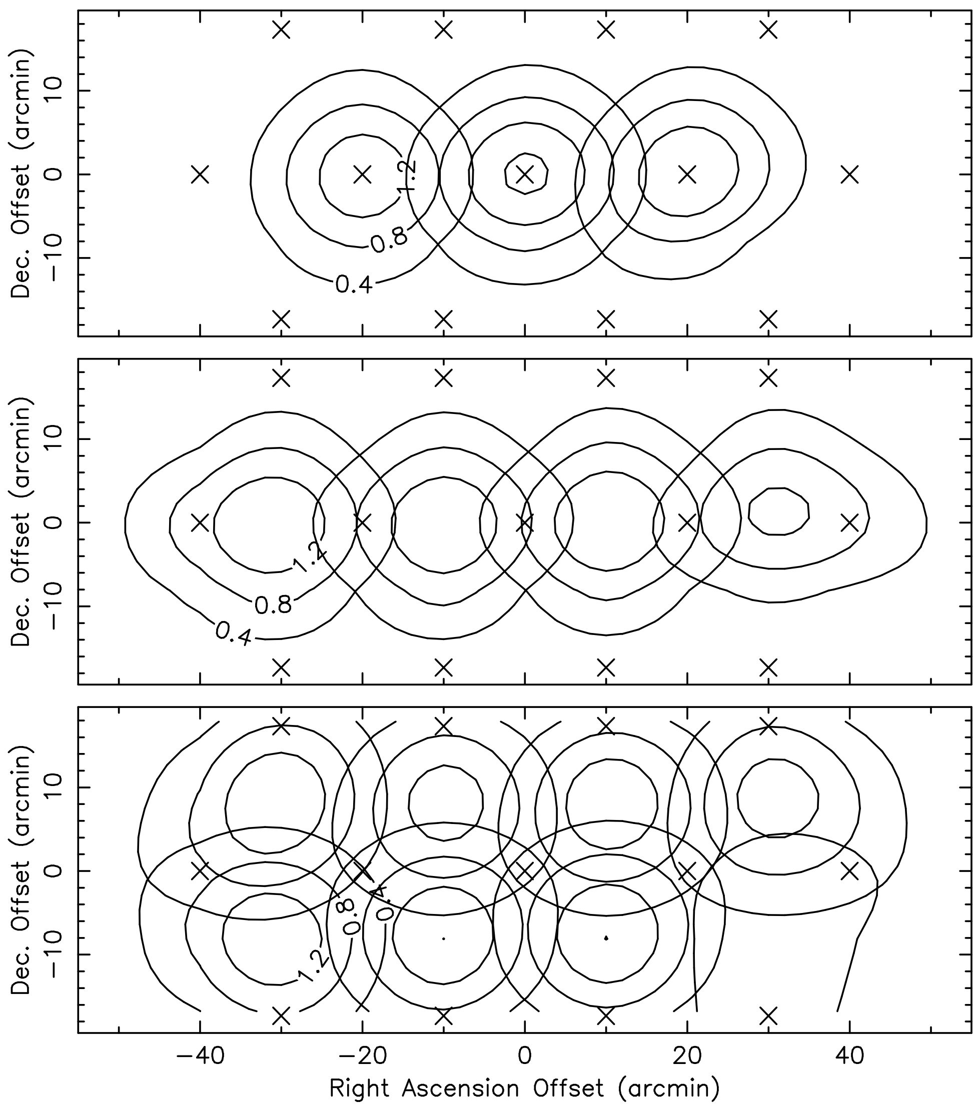

Figure 7. Beam maps with the the correlation data combined to form beams at various places in the array's field of view. The second highest contour is half peak intensity. The crosses mark beam locations that would center the focal spot on one of the array elements. Data from the lower right element was not recorded.